5B.2

4-Dimensional Variational Data Assimilation for the Weather Research and Forecasting Model

Xiang-Yu Huang[*1], Qingnong Xiao[1], Xin Zhang[2], John Michalakes[1], Wei Huang[1], Dale M. Barker[1], John Bray[1], Zaizhong Ma[1], Tom Henderson[1], Jimy Dudhia[1], Xiaoyan Zhang[1], Duk-Jin Won[3], Yongsheng Chen[1], Yongrun Guo[1], Hui-Chuan Lin[1], Ying-Hwa Kuo[1]

[1]National Center for Atmospheric Research, Boulder, Colorado, USA
[2]University of Hawaii, Hawaii, USA
[3]Korean Meteorological Administration, Seoul, South Korea

1. Introduction

The 4-dimensional variational data assimilation (4D-Var) (Le Dimet and Talagrand, 1986; Lewis and Derber, 1985) has been pursued actively by research community and operational centers over the past two decades. The 5th generation Pennsylvania State University – National Center for Atmospheric Research mesoscale model (MM5) based 4D-Var (Zou *et al.* 1995; Ruggiero *et al.* 2006), for example, has been widely used for more than 10 years. There are also successful operational implementations of 4D-Var (e.g. Rabier *et al.* 2000).

The 4D-Var technique has a number of advantages over 3-dimensional schemes including the abilities to:

1) Use observations at the almost exact times (to the width of the observation windows, see the discussion in the next section) that they are observed, which suits most asynoptic data,
2) Implicitly use flow-dependent background errors, which ensures the analysis quality for fast developing weather systems, and
3) Use a forecast model as a constraint, which enhances the dynamic balance of the final analysis.

The last mentioned advantage also implies that the current Weather Research and Forecasting model (WRF) based 3-dimensional variational data assimilation system (Barker *et al.* 2004b), which is developed from MM5 3D-Var (Barker *et al.* 2004a), should be enhanced with a 4-dimensional capability, using the WRF forecast model as a constraint, in order to provide the best initial conditions for the WRF model.

The 4D-Var component of the expanded 3/4D-Var system (known as WRF-Var, Barker *et al.* 2005), hereafter referred to as WRF 4D-Var, has undergone extensive development since 2004. It uses the WRF model and 3D-Var as its basic components (Huang *et al.* 2005).

* Corresponding author: Dr. Xiang-Yu Huang, NCAR/MMM, P.O. Box 3000, Boulder, CO 80307, USA. Email: huangx@ucar.edu

The 4D-Var prototype was built in 2005 and has under continuous refinement since then. Many single observation experiments have been carried out to validate the correctness of the 4D-Var formulation. A series of real data experiments have been conducted to assess the performance of the 4D-Var (Huang *et al.* 2006). Another year of fast development of 4D-Var has led to the completion of a basic system, which will be described in section 3.

2. The WRF 4D-Var Algorithm

The WRF 4D-Var follows closely the incremental 4D-Var formulation of Courtier *et al.* (1994), Veersé and Thépaut (1998), and Lorenc (2003). The data flow and program structure of WRF 4D-Var are given in Fig. 1.

The input to WRF 4D-Var is as the following. The observations are grouped into K windows, $\mathbf{y}_k$ ($k=1,K$). A short-range forecast is used as the background, $\mathbf{x}^{\mathbf{b}}$. The background error covariance matrix, $\mathbf{B}$, and the observation error covariance matrix, $\mathbf{R}$, are known by assumption. The lateral boundaries, WRFBDY, are required to integrate the WRF model over a time period. The 3D-Var solution can be obtained by setting K=1 and removing WRF model related components.

Both 3D-Var and 4D-Var techniques within WRF-Var include outer-loops and inner-loops. The outer-loops solve the nonlinear aspects of the assimilation problem, which for 4D-Var includes the integration of the full nonlinear model, while the inner-loops run a minimization algorithm for a quadratic problem. Using superscript $\mathbf{n}$ for the outer-loop index, the analysis vector, $\mathbf{x}^{\mathbf{n}}$, is the final output of WRF 4D-Var.

For the inner-loops, the minimization starts from a guess vector, $\mathbf{x}^{\mathbf{n-1}}$ (the analysis vector from the previous outer-loop). For the first outer-loop, $\mathbf{n}$=1, $\mathbf{x}^{\mathbf{b}}$ is normally taken as the guess vector, $\mathbf{x}^{\mathbf{0}}$. It should be stressed that in the incremental formulation the background vector and the guess vector should not be mixed. They are the same only during the first outer-loop.

Mathematically WRF 4D-Var minimizes a cost function J,

$$J = J_b + J_o + J_c \tag{1}$$

where J_b is the background constraint which penalizes the analysis towards the background, J_o is the observation constraint penalizing the analysis towards the observations, and J_c is the balancing constraint penalizing the analysis towards a balanced state. The J_c formulation implemented in WRF 4D-Var follows closely the form in Gustafsson (1992), Gauthier and Thépaut (2001), and Wee and Kuo (2004).

For the preconditioning, a variable transform,

$$\mathbf{v}^{\mathbf{n}} = \mathbf{U}^{-1}\left(\mathbf{x}^{\mathbf{n}} - \mathbf{x}^{\mathbf{n-1}}\right) \tag{2}$$

is chosen and the cost function gradient J' with respect to the control variable $\mathbf{v}^{\mathbf{n}}$ is

$$\begin{aligned} J'(\mathbf{v}^n) &= \sum_{i=1}^{n-1} \mathbf{v}^i + \mathbf{v}^n \\ &+ \mathbf{U}^T \mathbf{S}^T_{V\text{-}W} \sum_{k=1}^{K} \mathbf{M}_k^T \mathbf{S}^T_{W\text{-}V} \mathbf{H}_k^T \mathbf{R}^{-1} \left\{ \mathbf{H}_k \mathbf{S}_{W\text{-}V} \mathbf{M}_k \mathbf{S}_{V\text{-}W} \mathbf{U}\mathbf{v}^n - \mathbf{d}_k \right\} \\ &+ \mathbf{U}^T \mathbf{S}^T_{V\text{-}W} \sum_{i=0}^{N} \mathbf{M}_i^T f_i \, \gamma_{df} \mathbf{C}^{-1} \left(\sum_{i=0}^{N} f_i \, \mathbf{M}_i \mathbf{S}_{V\text{-}W} \mathbf{U}\mathbf{v}^n \right) \end{aligned} \tag{3}$$

where $\mathbf{B} = \mathbf{U}\mathbf{U}^T$ (Barker *et al.* 2005); superscripts -1 and T denote inverse and adjoint of a matrix or a linear operator; $\mathbf{d}_k$ are the innovation vectors for observation window k:

$$\mathbf{d}_k = \mathbf{y}_k - H_k \left\{ \mathbf{S}_{W-V} \left[M_k \left(\mathbf{x}^{n\text{-}1} \right) \right] \right\} \tag{4}$$

H_k, $\mathbf{H}_k$ and $\mathbf{H}_k^T$ are the nonlinear, tangent linear and adjoint observation operators over observation window k, which transform atmospheric variables between the gridded analysis space and observation space; M_k, $\mathbf{M}_k$ and $\mathbf{M}_k^T$ are the nonlinear, tangent linear and adjoint models, which propagate in time the guess vector $\mathbf{x}^{\mathbf{n-1}}$, analysis increments $\mathbf{U}\mathbf{v}^{\mathbf{n}}$ and analysis residual, (.) in Equation (3), respectively; $\mathbf{S}_{W\text{-}V}$, $\mathbf{S}_{V\text{-}W}$, $\mathbf{S}_{W\text{-}V}^{\ T}$ and $\mathbf{S}_{V\text{-}W}^{T}$ are the WRF 4D-Var specific operators which transform variables (e.g. between T and q) and grids (between A-grid and C-grid) between VAR and WRF$^+$; f_i is the modified coefficients for the digital filter (Lynch and Huang, 1992; Gauthier and Thépaut, 2001), γ_{df} is the weight assigned to J_c term.

WRF, WRF+, VAR and COM are the 4 major components of WRF 4D-Var in terms of software structure (Fig. 1):

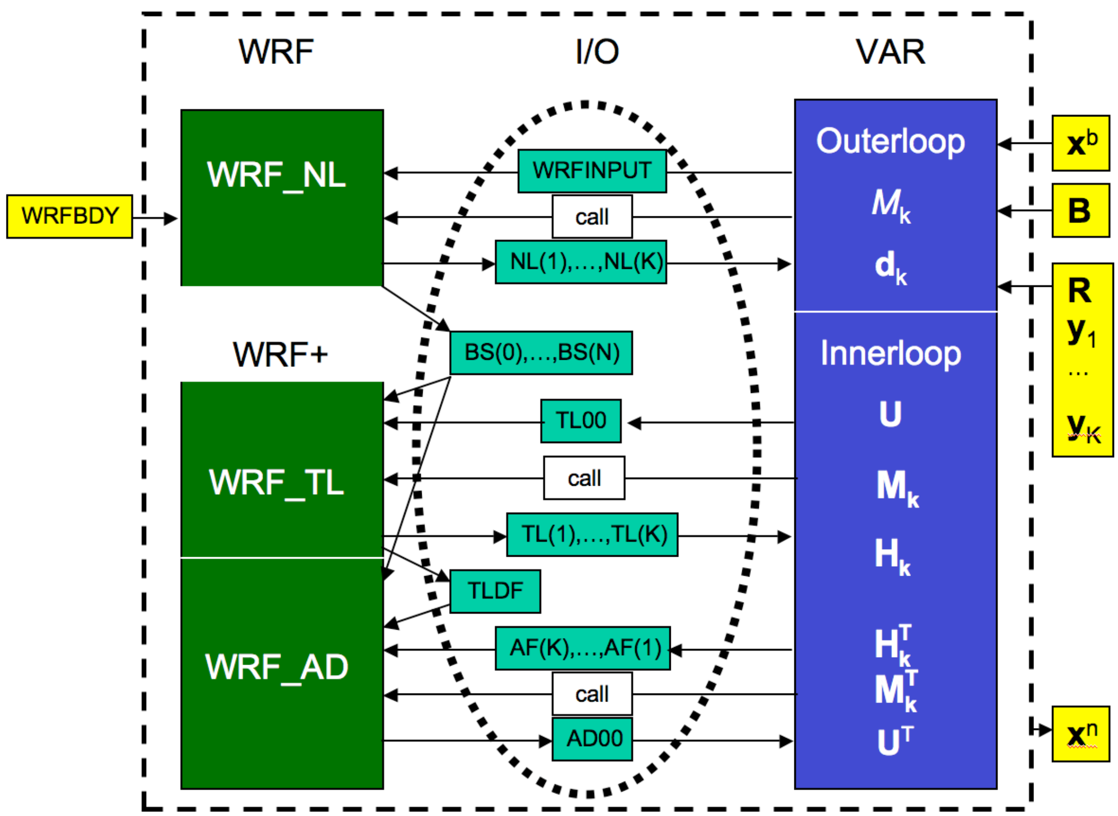

Fig. 1. The data flow and program structure of WRF 4D-Var.

I. WRF

The Advanced Research WRF model (ARW, Skamarock *et al*. 2005) is referred to here as WRF_NL. The ARW solves the compressible, nonhydrostatic Euler equations which are cast in flux form and conserve both mass and energy. The model has terrain-following vertical coordinate and Arakawa C-grid staggering horizontal grid. In addition to the wide range of physics options, the high-order numerical methods including a 3rd order Runge-Kutta time-split integration scheme and the 2nd to 6th order advection options make the ARW suitable for multi-scale numerical simulations and forecasts.

II. WRF$^+$

WRF$^+$ comprises two models in one framework, namely WRF tangent linear model (WRF_TL) and WRF adjoint model (WRF_AD), which are compiled together into a single executable. The Transformation of Algorithms in Fortran (Giering and Kaminski, 2003) is used to construct the tangent linear model and its adjoint from a simplified subset of nonlinear WRF model (WRF_NL). The tangent linear and adjoint codes passed the standard gradient tests and TL/AD tests following Zou *et al.* (1997). Sensitivities studies using WRF_AD have been carried out and reported by Xiao *et al.* (2007). Results in Section 4 may also be used as a check for the accuracy of WRF_TL.

III. VAR

VAR contains all the components of WRF 3D-Var (Barker *et al.* 2005) plus the 4-dimensional related enhancements. Among the enhancements are the grouping of observations (i.e., splitting $\mathbf{y}$ into $\mathbf{y_k}$) and their related calculations (replacing H, $\mathbf{H}$ and $\mathbf{H^T}$ by H_k, $\mathbf{H_k}$ and $\mathbf{H_k}^\mathbf{T}$) according to the observation windows (k); the calls to WRF_NL, WRF_TL and WRF_AD; and the grid/variable transform operators.

IV. COM

As WRF, WRF$^+$ and VAR are separate components, COM manages the communications among them. The implementation of COM is hidden from the other three components, allowing the movement of data to be handled either through disk I/O, or for maximum efficiency, through memory.

When the disk I/O is used, the following files are used for the communication:

WRFINPUT: the full model state at the beginning of each outerloop, written out by VAR and read in by WRF as initial model state;

NL(1),…,NL(K): K model states, one for each observation window, produced by WRF and read in by VAR before computing the innovation vector $\mathbf{d}_k$;

BS(0),…,BS(N): $N+1$ model states, one for each time step, produced by WRF and read in by WRF+ as basic states;

TL00: the initial model state for the tangent linear model, written out by VAR after the $\mathbf{U}$ and $\mathbf{S}_{V\text{-}W}$ transforms and read in by WRF+;

TL(1),…,TL(K): K (tangent linear) model states, one for each observation window, produced by WRF+ during the tangent linear integration and read in by VAR before computing the adjoint forcing (AF), defined below;

TLDF: the digital filter forcing [the last summation in Equation (3)],

$$\sum_{i=0}^{N} f_i \, \mathbf{M}_i \mathbf{S}_{V\text{-}W} \mathbf{U} \mathbf{v}^n \tag{5}$$

written out by WRF+ at the end of the tangent linear integration and read in by WRF+ at the beginning of the adjoint integration;

AF(K),…,AF(1): K files with AF for each observation window k,

$$\mathbf{S}_{W\text{-}V}^T \mathbf{H}_k^T \mathbf{R}^{-1} \left\{ \mathbf{H}_k \mathbf{S}_{W\text{-}V} \mathbf{M}_k \mathbf{S}_{V\text{-}W} \mathbf{U} \mathbf{v}^n - \mathbf{d}_k \right\} \tag{6}$$

written by VAR and read in by WRF+ during the adjoint integration;

AD00: the output of WRF+ after the adjoint model integration, read in by VAR before the $\mathbf{S}_{V\text{-}W}{}^T$ and $\mathbf{U}^T$ transforms.

3. The basic system

The WRF 4D-Var prototype was built in 2005. It has been under continuous refinement since then (Huang *et al.* 2006). Collaborative effort during the last year results in a basic system of WRF-Var (4D, version 2.2). It has the following features:

1) It runs as a combination of WRF (the released version 2.2), WRF+ (the WRF tangent linear model and adjoint model) and WRF-Var (the release version 2.1 with 4D-Var extensions) executables,
2) It uses system calls to invoke the three executables,
3) It uses disk I/O to handle the communication among WRF, WRF+ and VAR,
4) It can run on a single processor as well as multi-processors,
5) It has a penalty term, J_c, to control noise during the minimization, and
6) It includes a simple vertical diffusion with surface friction scheme and a large-scale condensation scheme in addition to the full dynamics in WRF+.

The parallel multiple program multiple data (MPMD) system architecture of WRF 4D-Var has demonstrated encouraging performance and made cycling data assimilation experiments possible.

Figure 2 shows a typical real-case example of the cost functions (J_o , J_b and J_c) evolving as functions of minimization simulations (iterations). For this particular case WRF 4D-Var reaches the minimum, defined as the gradient norm reduces to 1% of its original value, in about 40 iterations.

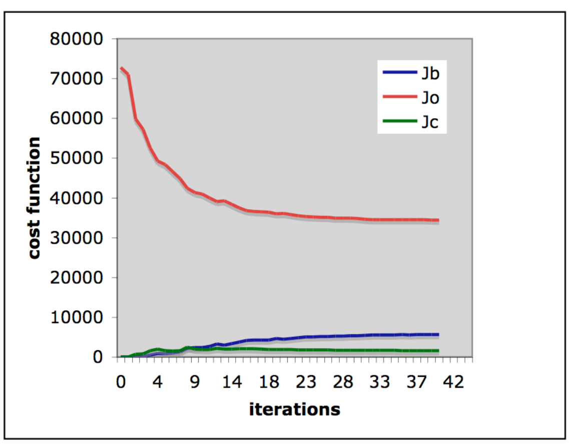

Fig. 2. The cost functions (J_b, J_o and J_c) as functions of minimization simulations (iterations).

4. WRF 4D-Var structure functions

Analysis increments due to a single observation produced by a data assimilation system implicitly provide structure functions or effective background error covariance matrix **B** (Thépaut *et al.* 1996). In order to compare the implicit structure function of WRF-Var in 3D-Var and 4D-Var mode, many single observation experiments are carried out. An example of these experiments is shown in this section.

The background, a 6-h forecast valid at 0000 UTC 25 Jan 2000, is used for both 3D-Var and 4D-Var. A single temperature observation at 0600 UTC is placed at (75 W, 30 N, 500 hPa). The case is constructed to demonstrate one of the potential problems related to 3D-Var when assimilating asynoptic observations. Although this case is constructed with a large time difference, the problem exists as long as the observation time differs from the analysis time.

The 3D-Var increments [the first panel (00h) of Fig. 3] show a Gaussian-like structure centered at the observation location. This is a graphic presentation of the background error covariance matrix, **B**, or 3D-Var structure function. The increments are added to the background at the analysis time to produce the 3D-Var analysis. Two forecasts using WRF are then made, one from the background and the other from the analysis. The differences between the two forecasts are shown in Fig. 3. In this particular case, as the observation time and analysis time are 6 hours apart. The changes made by 3D-Var assimilation of observation produce little impact of the model field at the time and location of the observations

The 4D-Var increments have a temporal dimension. They are shown in Fig. 4. The increments at 06 h (the last panel of Fig. 4) give a graphic representation of the background error covariance matrix at 06h, $\mathbf{MBM}^T$, or 4D-Var structure function. In addition to providing a fit to the observation at the observation location, it has a clear flow-dependent nature. The increments at the analysis time (00 h), the first panel of Fig. 4, are small with a center upstream of the observation. The 4D-Var analysis is obtained by adding the increments at 00 h to the background. Again, the differences between the two forecasts, one from the background and the other from the 4D-Var analysis are shown in Fig. 5. The 6-h forecast from the 4D-Var analysis provides a better fit to the observation. The fact that the potential temperature increments in Fig. 4 and the forecast differences in Fig. 5 are similar suggests that the linear approximations in 4D-Var are reasonable for this case.

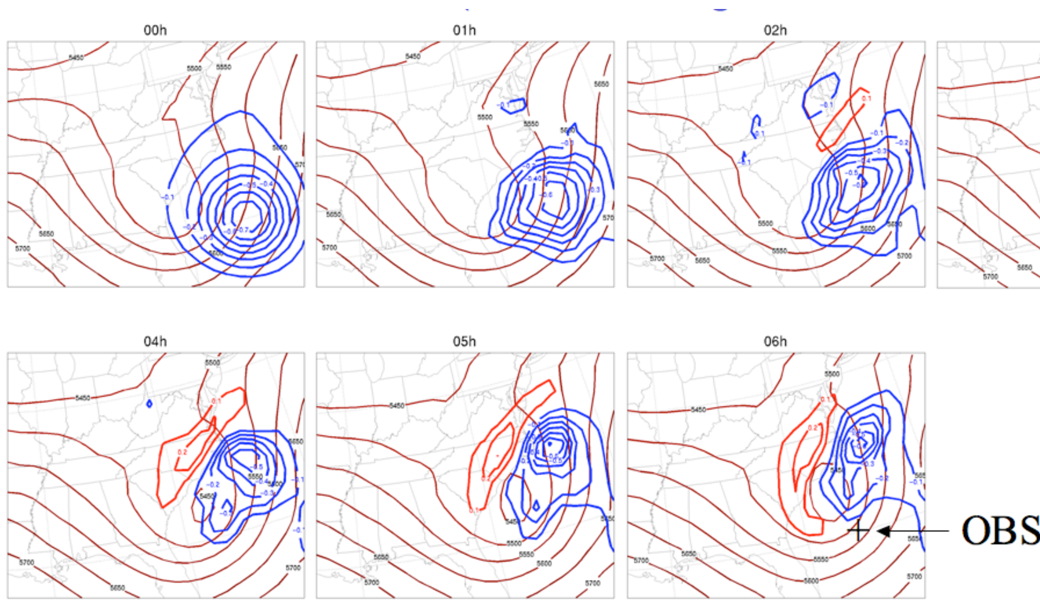

Fig. 3. The differences of the potential temperature (red/blue contours) at 500mb at 00,01,02,03,04,05,06h from two forecasts, one initialized from the background and the other from the 3D-Var *analysis. The brown contours are geopotential height in the forecast from the background. + indicates the observation location.*

5. Cold start experiments

To assess the 4D-Var performance and to test it in a near operational configuration, a series of experiments have been conducted on Typhoon Haitang, which hit Taiwan on 0000 UTC 18 July 2005 (Guo *et al.* 2006).

Five sets of forecast experiments are performed. Each set has nine 48-h forecasts initialized at nine different *analysis times* starting from 0000 UTC 16 July (denoted as 1600) to 0000 UTC 18 July (1800) with 6-h apart. Five sets of forecasts differ by their initial conditions described as following:

FGS – forecast initialized from National Center for Environment Prediction (NCEP) Global Forecast System (GFS) analysis 6-h earlier from the analysis time. Its 6-h forecast serves as the background field or first guess for other data assimilation experiments.

AVN- forecast from the NCEP GFS analysis

3DVAR – forecast from the 3D-Var analysis

FGAT – forecast from a First Guess At Appropriate Time (FGAT) analysis [an option of 3D-Var, see Lee and Barker (2005) and Huang *et al.* (2005)]

4DVAR – forecast from the 4D-Var analysis

The same parameter set and physics options are used for all forecast runs. The model domain has 91x73x17 grid points with a 45 km horizontal spacing and 4-min time step.

The assimilated observations include conventional data, satellite data and bogus data from the Central Weather Bureau of Taiwan. Table 1 lists the numbers of different observation types in a 6-h time window, from 0000 UTC and 0600 UTC 16 July. At other analysis times, there are also GPS refractivity (*N*) data and QuikScat wind (*QS-u, QS-v*) data (e.g. 212 *N*, 2594 *QS-u* and 2605 *QS-v* at 0600 UTC 16 July).

Table 1. The numbers of different observation types assimilated by 4D-Var at 0000 UTC 16 July.

Obs type	*u*	*v*	*T*	*p*	*q*	*DZ*
TEMP	727	724	869		697	
SYNOP	119	218	237	226	236	
SATOB	3187	3182				
AIREP	923	930	939			
PILOT	156	160				
METAR	167	191	216		200	
SHIP	69	70	77	79	73	
SATEM						511
BUOY	67	67		64		
BOGUS	1200	1200	788	788	80	

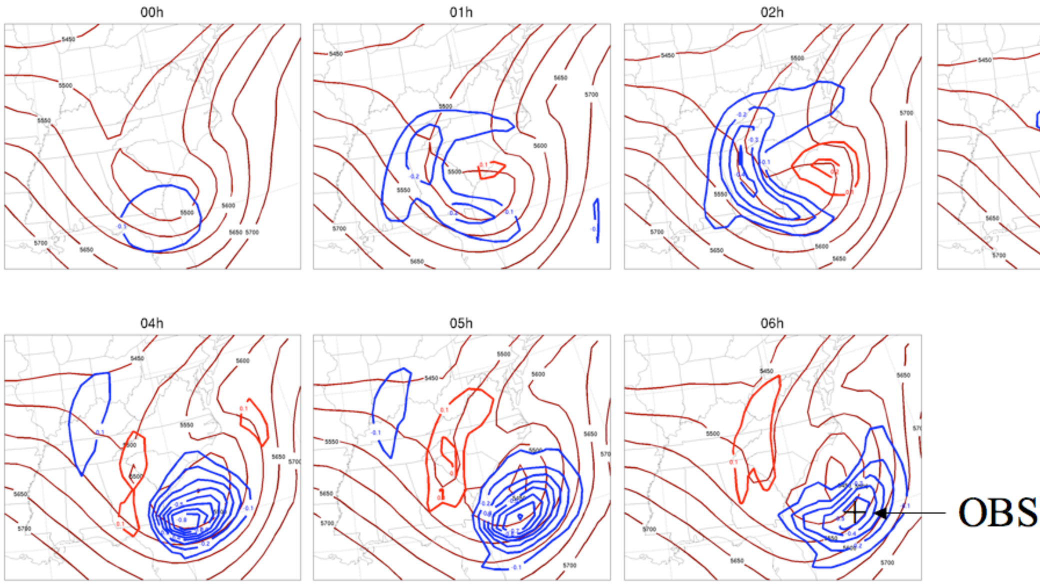

Fig. 4. Potential temperature increments at500mb at 00,01,02,03,04,05,06h to a temperature observation at 500mb at 06h. + indicates the observation location.

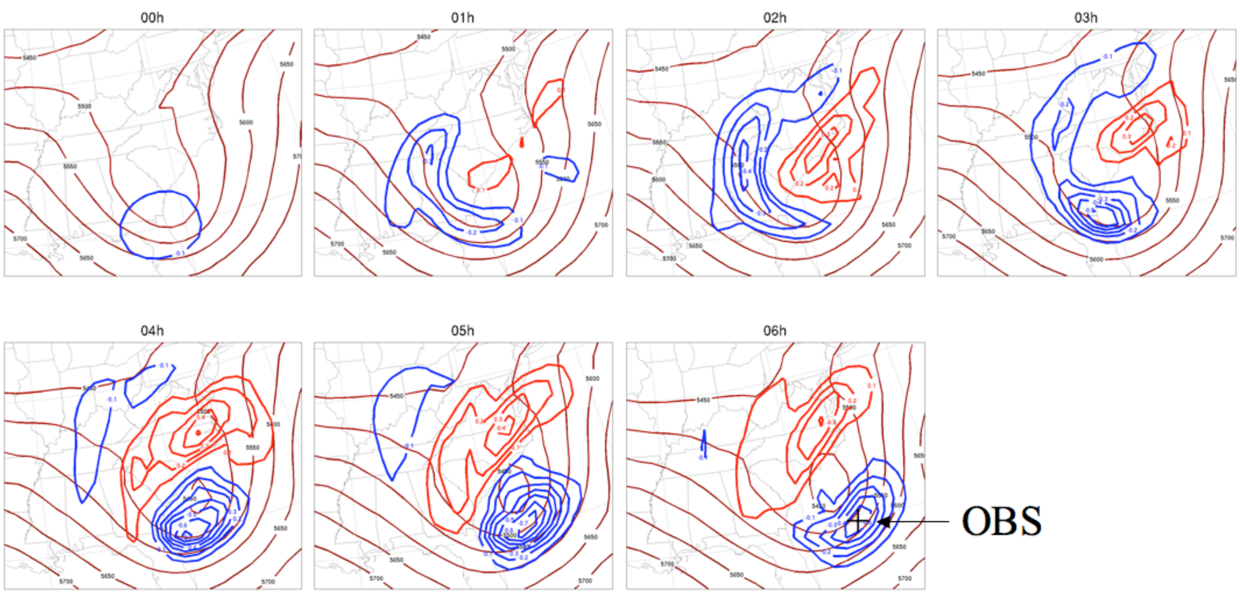

Fig. 5. Same as Fig. 3, but for the difference between a forecast initialized from the 4D-Var analysis and from the background.

The 48-h forecasts of the typhoon track, all started at 0000 UTC 16 July 2005, are plotted in Fig. 6, together with the observed track. The background sea level pressure field at initial time is also shown in the figure. The forecast initialized from FGS is the worst. The forecasts from AVN, 3DVAR and FGAT are of similar quality. The 4DVAR analysis leads to the best track forecast.

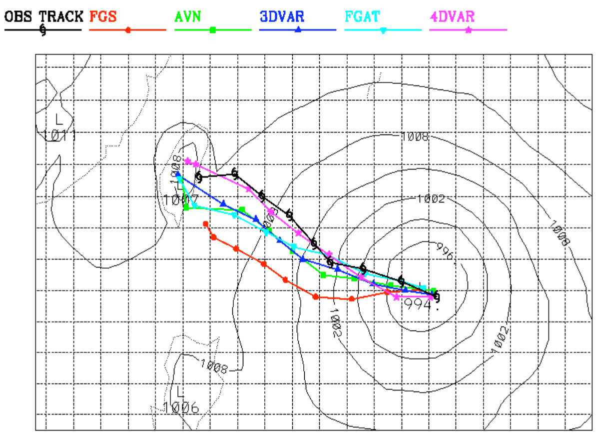

Fig. 6. 48-h forecast typhoon tracks from FGS, AVN, 3DVAR, FGAT, 4DVAR, together with the observed track. Forecasts are all made from 0000 UTC 16 July 2005. The background sea level pressure field from FGS is also shown.

The track forecast errors in km averaged over the 48-h forecast range are listed in Table 2. The best forecast at each analysis time is highlighted. It is evident that 4D-Var produces superior track forecast for Typhoon Haitang over the 2-day period.

Table 2. The track forecast errors in km averaged over 48 h for each forecast.

Time	FGS	AVN	3DVAR	FGAT	4DVAR
1600	159	85	72	77	**66**
1606	108	83	**67**	97	79
1612	93	100	95	**82**	137
1618	116	67	103	**52**	54
1700	80	66	68	62	**52**
1706	83	80	80	67	**65**
1712	111	104	**90**	112	128
1718	113	113	133	129	**93**
1800	116	221	192	**103**	111
Mean	109	102	100	**87**	**87**

Up to now, only the typhoon track forecasts have been investigated. Other aspects of the analyses and forecasts will also be studied and reported in the near future. Observing system experiments will be carried out to assess the impact of different observation types, in particular, the vortex bogus observations (Guo *et al.*, 2006).

6. Cycling experiments

A 4.5-day period from 12 UTC 4 May to 00 UTC 9 May 2006 was chosen for assessing the impact of data assimilation using 3D-Var and 4D-Var in cycling mode on the forecast. During this time period, a cyclone moved from the west sea cross the Korean peninsula and caused heavy precipitations.

In these experiments, the model domain is the same as that of the current Korea Meteorological Administration (KMA) regional numerical prediction system, but the horizontal resolution is reduced to 30 km with 60x54x31 grid points. The analysis is done every 6-h followed by a 24-h forecast over this 4.5-day period. In cycling mode, the analysis uses the 6-h forecast from the previous analysis as the background, except at the very beginning of the experiment when the initial model states are obtained by interpolating the 30-km operational model fields.

Two sets of experiments are run over the 4.5-day period:

3DVAR: 3D-Var is used with the interpolated model state as the background. Observations collected from -3h to +3h around the analysis time are assimilated; an example of the numbers of different observations is given in Table 3.

4DVAR: 4D-Var is used. The interpolated model state valid at 6 h before the analysis time is used to make a 3-h forecast. This 3-h forecast is then used as the background for 4D-Var analysis. Observations collected from -3h to +3h around the analysis time are split to hourly time slots. The observations used in one 4DVAR analysis are given in Table 4. Due to the data thinning strategy, 4DVAR uses significantly more SYNOP and METAR observations. There was a small error in the 4DVAR experiment, which excludes all SATOB observations. After 4DVAR analysis valid at -3h, another 3-h forecast is run to advance the model state to the analysis time. The model lateral and lower boundaries are updated at -3h and at the analysis time.

The performance of 4DVAR is evaluated using 3DVAR as a reference. As this is a major precipitation case, the precipitation forecast is verified.

Table 3 Number of Observations used by 3D-Var on 2006050412.

	u	v	T	p	q
TEMP	459	464	519	-	385
SYNOP	67	59	73	71	72
SATOB	74	76	-	-	-
PILOT	182	195	-	-	-
METAR	559	551	614	33	36
SHIP	1	1	2	2	1

Precipitation skill scores are calculated and averaged over 7 days at 73 observation points in South Korea. The scores are defined as following:

Hit (H) event forecast to occur AND did occur
Miss (M) event forecast not to occur BUT did occur
False_alarm (F) event forecast to occur BUT did not

Table 4 Number of Observations used by 4DVAR on 2006050412.

	u	v	T	p	q
TEMP	456	461	519	-	384
SYNOP	253	212	268	191	204
SATOB	-	-	-	-	-
PILOT	185	194	-	-	-
METAR	2636	2402	2957	218	240
SHIP	1	1	2	2	1

Critical Success Index (CSI) = H / (H + M + F)

The precipitation scores, CSI of 0.1mm, 5mm, 15mm and 25mm are showed in Fig. 7. The Precipitation forecasts in the 4DVAR experiments over the 4.5-day period are significantly better than the 3DVAR experiments.

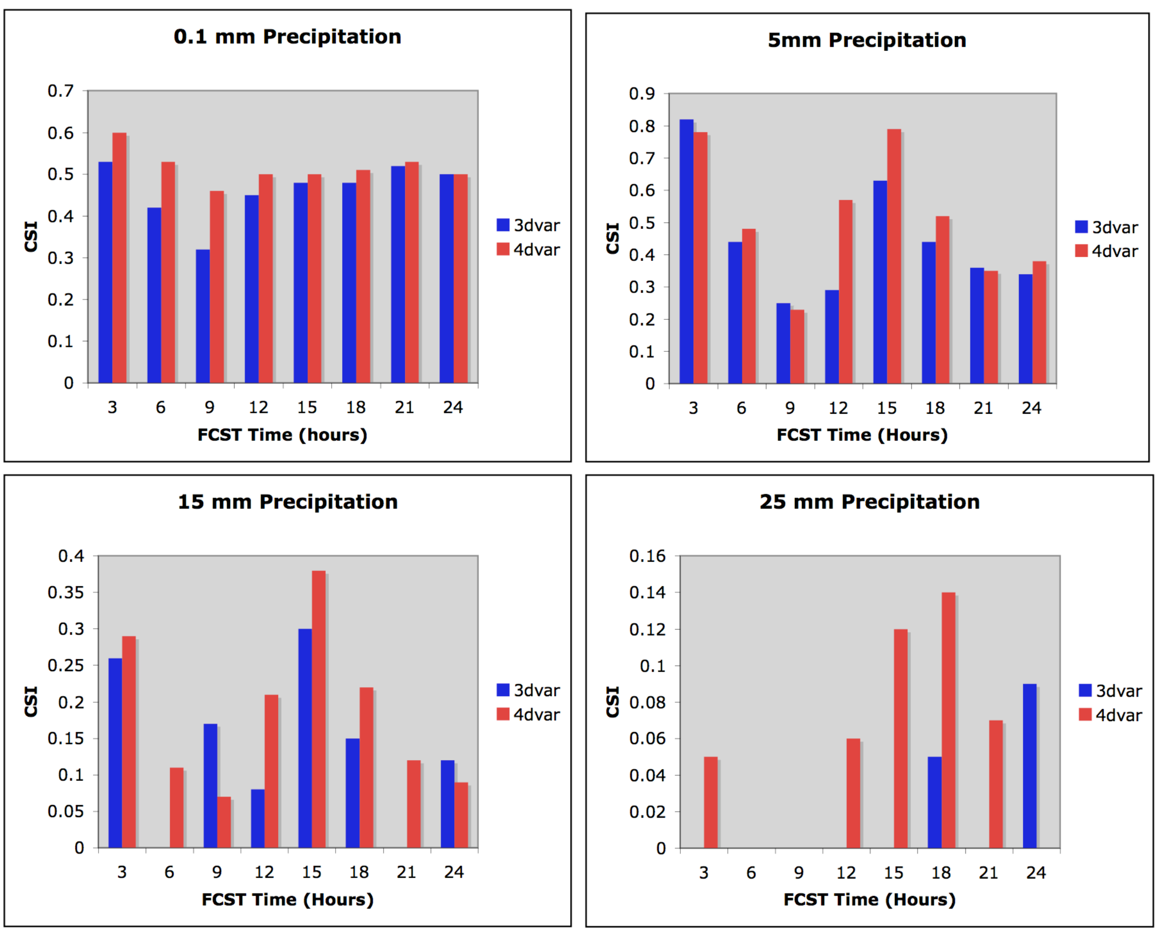

Fig. 7. Precipitation Verification: 0.1mm, 5mm, 15mm, 25 mm Precipitation.

7. Conclusions

In this paper, a brief overview of the 4D-Var capability within WRF-Var is given. The WRF 4D-Var has been built on the multi-incremental formulation of WRF-Var. The current status of the WRF 4D-Var is characterized by the basic system which uses multiple executables, can run on a single processor as well as multiple processors and uses disk I/O to handle the communication among the executables.

The structure functions of the 4D-Var are studied using single observation experiments. The example showed in this paper clearly demonstrates the flow-dependent nature of the analysis increments in 6-h assimilation window: a small increment upstream of the observation at the beginning of the assimilation window; the intensification of the increment in time; and the final increment centered at the observation location with the structure stretched along the mean flow. Comparison between the structure function and the difference of nonlinear runs provides us with a powerful tool for checking the code correctness and the linearization validity made in deriving the tangent linear and adjoint models.

Many cold start real data experiments have been conducted, as they can run on single processor and do not require a supercomputer. Within the WRF-Var framework, 4D-Var can assimilate most observation types as 3D-Var does, and it can assimilate more observations from non-moving platforms, such as SYNOP, than 3D-Var. The results indicate that 4D-Var is working properly and, on the average, outperforms 3D-Var with a similar configuration.

Cycling experiments have just become possible with recent development of the parallel multiple programs multiple data system architecture of WRF 4D-Var. Preliminary results are encouraging and in agreement with those from the cold start experiments. Further experiments and evaluation are on going.

The current WRF 4D-Var has a simple vertical diffusion scheme and a large-scale condensation scheme, in addition to the full WRF dynamics, in the tangent linear and adjoint models. As high impact weather prediction is receiving more and more attention in recent years, further studies will be conducted to assess the impact of 4D-Var on WRF forecasts of severe weathers, such as heavy rainfall events, tropical cyclones, and so on. It is obvious that more physics should be added in the tangent linear and adjoint models of WRF 4D-Var.

There are many tunable parameters in WRF-Var, for example the variances and scale lengths of the background errors. Most of these parameters have been tuned for optimizing the 3D-Var performance. In all the 4D-Var experiments conducted so far, none of these parameters have been touched. Extensive tuning experiments are necessary and planned. Results will be reported in the near future.

Acknowledgments

The 4D-Var development for WRF has been primarily supported by the Air Force Weather Agency and the Korea Meteorological Administration.

References

Barker, D.M., W. Huang, Y.-R. Guo, A.J. Bourgeois, Q.N. Xiao, 2004a: A three-dimensional variational data assimilation system for MM5: Implementation and initial results. *Mon. Wea. Rev.*, **132**, 897-914.

Barker, D. M., M.S. Lee, Y. -R. Guo, W. Huang, Q. -N. Xiao, and S. R. H. Rizvi, 2004b: WRF Variational Data Assimilation Development at NCAR. WRF Workshop, June 2004.

Barker, D. M., Y. -R. Guo, W. Huang, S. R. H. Rizvi, Q. -N. Xiao, Y.- H. Kuo, J. Gu, X. -Y. Huang, and M. -S. Lee, 2005: WRF-Var - A Unified Variational Data Assimilation System For WRF. WRF Workshop, June 2005.

Courtier, P., J.-N. Thépaut, and A. Hollingsworth, 1994: A strategy for operational implementation of 4D-Var, using an incremental approach. *Quart. J. Roy. Meteor. Soc.*, **120**, 1367-1387.

Gauthier, P. and J.-N. Thépaut, 2001. Impact of the digital filter as a weak constraint in the preoperational 4DVVR assimilation system of Météo France. *Mon. Wea. Rev.*, **129**, 2089-2102.

Giering, R., and T. Kaminski, 2003: Applying TAF to generate efficient derivative code of Fortran 77-95 programs. *PAMM*, **2(1)**, 54-57.

Guo, Y.R., H.-C. Lin, X. X. Ma, X.-Y. Huang, C.T. Terng, and Y.-H. Kuo, 2006. Impact of WRFVar (3DVar) Background Error Statistics on Typhoon analysis and Forecast. WRF users' workshop, Boulder, Colorado, 19-22 June 2006.

Gustafsson, N. 1992. Use of a digital filter as weak constraint in variational data assimilation. Workshop proceedings on Variational assimilation, with special emphasis on three-dimensional aspects. Pp 327-338. Availabel from ECMWF.

Huang, X.-Y., Q. Xiao, W. Huang, D. Barker, Y.-H. Kuo, J. Michalakes, Z. Ma, 2005: The weather research and forecasting model based 4-dimensional variational data assimilation system. WRF/MM5 users' workshop, Boulder, Colorado, 27-30 June 2005.

Huang, X.-Y., Q. Xiao, W. Huang, D. Barker, J. Michalakes, J. Bray, Z. Ma, Y. Guo, H.-C.Lin, Y.-H. Kuo, 2006: Preliminary results of WRF 4D-Var. WRF users' workshop, Boulder, Colorado, 19-22 June 2006.

Lee, M.-S., and D. Barker, 2005: Preliminary Tests of First Guess at Appropriate Time (FGAT) with WRF 3DVAR and WRF Model, *J. Korean Met. Soc.* **41**, 495-505.

Le Dimet, F. and O. Talagrand, 1986: Variational algorithms for analysis and assimilation of meteorological observations: theoretic aspects. *Tellus*, **38A**, 97-110.

Lewis, J. and J. Derber, 1995: The use of adjoint equations to solve a variational adjustment problem with advective constraints. *Tellus*, **37A**, 309-327.

Lorenc, A.C. Modelling of error covariances by 4D-Var data assimilation. *Quart. J. Roy. Meteor. Soc.*, **129**, 3167-3182.

Lynch. P and Huang, X.-Y. 1992. Initialization of the HIRLAM model using a Digital Filter. Mon. Wea. Rev. 120, 1019-1034.

Rabier, F., H. Järvinen, E. Klinker, J.-F. Mahfouf and A. Simmons. 2000: The ECMWF operational implementation of four dimensional variational assimilation. *Quart. J. Roy. Meteor. Soc.*, **126**, 1143-1170.

Ruggiero, F. H., J. Michalakes, T. Nehrkorn, G. D. Modica, and X. Zou, 2006: Development of a New Distributed-Memory MM5 Adjoint. J. Atmos. Ocean. Technol., 23, doi: 10.1175/JTECH1862.1, 424-436.

Skamarock, W. C., J. B. Klemp, J. Dudhia, D. O. Gill, D. M. Barker, W. Wang and J. G. Powers, 2005: A Description of the Advanced Research WRF Version 2. NCAR Technical Note TN-468+STR. 88 pp.

Thépaut, J.-N., P. Courtier, G. Belaud and G. Lemaitre, 1996: Dynamic structure functions in a four-dimensional variational assimilation: A case study. *Quart. J. Roy. Meteor. Soc.*, **122**, 535-561.

Veersé, F. and J.-N. Thépaut, 1998: Multi-truncation incremental approach for four-dimensional variational data assimilation. *Quart. J. Roy. Meteor. Soc.*, **124**, 1889-1908.

Wee, T.-K., and Y.-H. Kuo, 2004: Impact of a digital filter as a weak constraint in MM5 4DVAR. *Mon. Wea. Rev.*, **132**, 543-559.

Xiao, Qingnong, Y.-H. Kuo, Z. Ma, Wei Huang, Xiang-Yu Huang, X.-Y. Zhang, D. M Barker, and J. Michalakes, 2007: Development of the WRF adjoint modeling system and its application to the investigation of the May 2004 McMurdo Antarctica severe wind event. *Mon. Wea. Rev*., submitted.

Zou, X., Y.-H. Kuo, and Y.-R. Guo, 1995: Assimilation of atmospheric radio refractivity using a nonhydrostatic mesoscale model. *Mon. Wea. Rev*., **123**, 2229-2249.

Zou, X., F. Vandenberghe, M. Pondeca and Y.-H. Kuo, 1997: Introduction to adjoint techniques and he MM5 adjoint modeling system. NCAR Tech. Note NCAR/TN-435-STR, 110pp.